Coupled Map Networks

José Koiller[1]‡ **and Lai-Sang Young**[2]§

[1] IMPA, Est. D. Castorina, 110, Rio de Janeiro, RJ 22460, Brazil.
[2] Courant Institute of Mathematical Sciences, New York University, 251 Mercer St, New York, NY 10012, USA.

E-mail: `koiller@impa.br` and `lsy@cims.nyu.edu`

Abstract. This paper discusses coupled map networks of arbitrary sizes over arbitrary graphs; the local dynamics are taken to be diffeomorphisms or expanding maps of circles. A connection is made to hyperbolic theory: increasing coupling strengths leads to a cascade of bifurcations in which unstable subspaces in the coupled map systematically become stable. Concrete examples with different network architectures are discussed.

AMS classification scheme numbers: 37D30, 37D50, 37L60

1. Introduction

This paper is about a class of multi-component dynamical systems we will refer to as *coupled map networks* (CMN). Roughly speaking, a CMN is characterized by local dynamics operating at each vertex or node of a graph, with these small constituent systems interacting along the edges of the graph. That CMNs are useful in applications is beyond doubt: they appear naturally in models in engineering (e.g., electronic circuits), in the physical and biological sciences (e.g., chemical reactions, genetic regulatory networks, neuronal networks) and as various agent-based models in the social sciences. These systems have also been studied from many different angles in the mathematical literature, both pure and applied, ranging from coupled oscillator networks to coupled map lattices. In a subject as vast and diverse as this one, without substantially reducing its scope it is impossible to do justice to the literature through a reasonable number of citations. We will from here on confine our discussion to dynamical models closer to ours.

This paper contains a mathematical study of discrete-time CMNs over arbitrary finite graphs. To keep the local dynamics simple yet nontrivial, we take them to be maps of a circle, such as rotations or expanding maps (simulating chaotic behavior), and the coupling is taken to be a form of averaging (to simulate a diffusion). Our models are therefore a close cousin of a much studied class of dynamical systems called *coupled map lattices* (CML), which are discrete-time models of generalized reaction-diffusion processes on homogeneous media [1, 2, 3, 4, 5, 6, 7, 18, 19, 20, 23, 24, 25, 28, 32]; see also [11] and the references therein. In a CML, the graph is a regular lattice, usually $\mathbb{Z}$ or $\mathbb{Z}^d$, and the couplings, nearest neighbor or finite range, are usually

assumed to be translationally invariant. By contrast, there is nothing homogeneous about our network connections or coupling strengths, and one of the purposes of this paper is to give concrete examples to demonstrate the wide range of dynamical behaviors that arise from different network architectures.

Very weak coupling regimes were studied in great detail in a number of CML papers related to ours (e.g., [7, 18, 23, 24]). The present paper differs in that we allow a wide range of coupling strengths and study how they affect the dynamics. In this regard, our paper is closer in spirit to [12] and [22]. Consider, for example, the case of expanding local maps. Clearly, a weakly coupled system continues to be expanding, but since averaging properties of the interaction translates into contraction for the CMN (this will be made precise in the text), contractive directions appear as coupling strengths are increased. Using an especially simple coupling, we show that as we tune our coupling strengths up gradually, one sees a cascade of bifurcations in which expanding subspaces systematically switch over to contractive subspaces, that is to say, the system goes from expanding to hyperbolic or partially hyperbolic, acquiring more and more contracting directions as the coupling gets stronger. While connections to hyperbolic theory were noted before, the transparency of this connection has never been brought out in the generality considered here. This connection also provides hyperbolic theory with an abundance of natural examples.

To be precise, our models are not exactly hyperbolic or partially hyperbolic but *piecewise* hyperbolic or partially hyperbolic, the discontinuities coming from the very simple coupling we use. As is well known to be the case, discontinuities in a dynamical system in dimensions greater than one can complicate dynamical behavior and lead to intriguing geometry [8, 9, 10, 13, 14, 16, 27, 30, 31]. We begin to touch upon these types of questions only in Section 5, where we point out some key differences in geometry of the attracting set for different coupling graphs.

To summarize, our aims in this paper are twofold. One is to remind mathematicians in the dynamical systems community of this useful and interesting class of models called CMNs which appears to be fertile ground for future research. The second is to provide examples and discuss some basic issues. In a sequel, the first-named author will discuss in greater depth the ergodic theory of a subset of these systems, including the existence of physical measures.

2. Setting and preliminaries

We define a *coupled map network* (CMN) to be a triple $(G, \{f_i\}, A)$ where

- G is a graph specified by a finite or countable set Ω of vertices and a collection of edges $\mathcal{E} \subset \Omega \times \Omega$;
- at each $i \in \Omega$, which we call a site, there is a *local space* X_i and a *local map* $f_i : X_i \to X_i$; and
- network dynamics are defined by the iteration of $\Phi : X \to X$ where $X = \prod_{i \in \Omega} X_i$ is the product space and $\Phi = A \circ F$ where $F = \prod_{i \in \Omega} f_i$ is the (independent) application of local maps and $A : X \to X$ is the spatial interaction or coupling; for $x = (x_i)_{i \in \Omega} \in X$, the i-th coordinate of $A(x)$ depends only on x_i and those x_j for which $(j, i) \in \mathcal{E}$.

This paper is about CMNs of the following type: G is an arbitrary *finite* graph with d vertices, and the local systems $f_i : X_i \to X_i$ are smooth circle maps, so that the global phase space X is the d-dimensional torus $\mathbb{T}^d$. Our couplings are averaging

operators intended to simulate diffusive behavior. The purpose of this section is to make precise the setting for our results.

In the definitions to follow, the local maps f_i play no role, and the focus is almost entirely on the coupling operator $A : X \to X$. We begin with the $d = 2$ case to provide motivation and introduce notation. The general definition is given in Section 2.2, and further properties of the coupling operator are discussed in Section 2.3.

2.1. Coupling of two maps

We let $\mathbb{S}^1 \equiv \mathbb{R}/\mathbb{Z}$, and use additive notation on $\mathbb{S}^1$. The aim of this subsection is to introduce a class of admissible couplings for two maps $f_i : \mathbb{S}^1 \to \mathbb{S}^1$, $i = 1, 2$. The following is one of the simplest rules for how to bring pairs of points in $\mathbb{S}^1$ closer: Fix a number α, say $\alpha = \frac{1}{3}$. For $x, y \in \mathbb{S}^1$, we move x a third of the way toward y along the shorter arc connecting x and y, to a point called x', and move y to y', which lies a third of the way toward x. The averaging map is then defined to be $A(x, y) = (x', y')$ (see Figure 1(a,b)). One sees immediately that there is a difficulty when x and y are antipodal: they cannot decide which direction to move (Figure 1(c)). In other words, this rule is not defined for antipodal points.
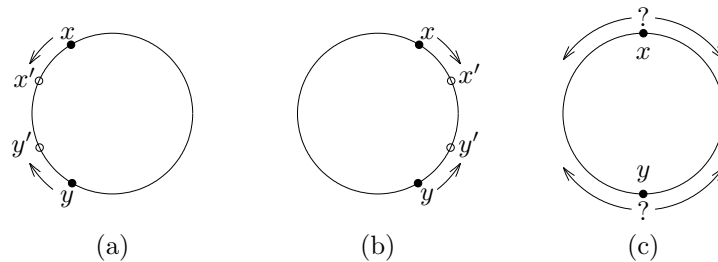

Figure 1. The averaging map $(x', y') = A(x, y)$. In (c), $A(x, y)$ is undefined.

There are many ways around this. For example, the strength of attraction α can be taken to be a function of $\operatorname{dist}_{\mathbb{S}^1}(x, y)$, the distance between x and y measured along $\mathbb{S}^1$, tapering off to zero as $\operatorname{dist}_{\mathbb{S}^1}(x, y) \to 1/2$. Different couplings will lead to different dynamical properties and technical considerations. As we will see in the next section, the linear coupling above is in many ways the simplest, and this is what we will use in this paper.

More formally, let $P = \{ (x, y) \in \mathbb{T}^2 \; ; \; \operatorname{dist}_{\mathbb{S}^1}(x, y) = 1/2 \}$. Given any *coupling strength* $\alpha > 0$, we define the coupling map $A : \mathbb{T}^2 \setminus P \to \mathbb{T}^2$ by setting

$$A(x, y) = \big(x + \alpha \lfloor y - x \rfloor, \, y + \alpha \lfloor x - y \rfloor \big) \quad \mathrm{mod} \ (1, 1), \tag{1}$$

where $\lfloor z \rfloor \in (-1/2, 1/2)$ is such that $\lfloor z \rfloor = z \bmod 1$ and "mod $(1,1)$" is shorthand for taking each coordinate mod 1. (Notice that for $z = 1/2 \bmod 1$, $\lfloor z \rfloor$ is not defined — and not needed — in (1).) Intuitively, $\lfloor y - x \rfloor$ measures the "oriented distance" from x to y in $\mathbb{S}^1$. In figure 1(a), $\lfloor y - x \rfloor > 0$, and in 1(b), $\lfloor y - x \rfloor < 0$.

The parameter α measures the strength of the coupling between the two local maps. The case $\alpha = 0$, which we do not consider, corresponds to f_1 and f_2 being uncoupled, i.e., Φ is the product map. When $\alpha = 1/2$, Φ collapses $\mathbb{T}^2$ onto the diagonal $\{x = y\}$, i.e., the two local maps are fully synchronized in one step, and effectively function as a single one-dimensional map from then on. For $\alpha > 1/2$, the analogy between (1) and a diffusion process breaks down; see Figure 2. In this paper

we will limit our attention to $\alpha \in (0, 1/2)$, and write A_α where necessary to make the dependence on α explicit.
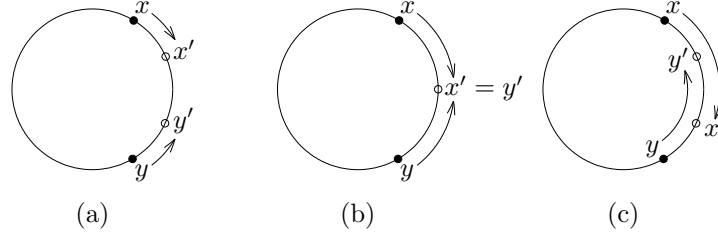
Figure 2. Behavior of A_α for different values of α. For $0 < \alpha < 1/2$, A_α behaves as in (a); for $\alpha = 1/2$, as in (b). If $\alpha > 1/2$, A_α no longer behaves as a diffusion process; it "overshoots" as in (c).

Since A is not defined on P, the coupled map $\Phi = A \circ F$ is not defined on $S = F^{-1}(P)$, and we have only $\Phi : \mathbb{T}^2 \setminus S \to \mathbb{T}^2$. We call S the *singularity set* of Φ.

2.2. General case

We assume throughout that (i) G is a *connected* graph with vertices or *sites* $\Omega = \{1, 2, \ldots, d\}$, (ii) no site is connected to itself, i.e., $(i, i) \notin \mathcal{E}$ for all i, and (iii) the edges are not oriented, i.e., for all $i, j \in \Omega$, $(i, j) \in \mathcal{E}$ if and only if $(j, i) \in \mathcal{E}$. To each $(i, j) \in \mathcal{E}$ we assign a number $c_{ij} = c_{ji} > 0$ which represents the coupling strength between sites i and j. If $(i, j) \notin \mathcal{E}$, $i \neq j$, we set $c_{ij} = 0$; and for $i = j$, we set

$$c_{ii} = 1 - \sum_{j \neq i} c_{ij}, \quad \text{for } i = 1, 2, \ldots, d;$$

the reason for this choice will become clear shortly. The symmetric $d \times d$ matrix $C = (c_{ij})$ thus obtained is called the *coupling matrix*. Note that, ignoring diagonal entries, C can be regarded as a weighted incidence matrix for the coupling graph G. Clearly, the matrix C contains all the information given by the graph G and more: for $i \neq j$, $c_{ij} > 0$ if and only if $(i, j) \in \mathcal{E}$.

Given a $d \times d$ coupling matrix C, we define the averaging map A_C as follows. Let

$$P(C) = \bigcup \{ P_{ij} ; (i, j) \in \mathcal{E} \} \quad \text{where} \quad P_{ij} = \{ x \in \mathbb{T}^d ; \text{dist}_{\mathbb{S}^1}(x_i, x_j) = 1/2 \}, \tag{2}$$

and define $A_C : \mathbb{T}^d \setminus P(C) \to \mathbb{T}^d$ by

$$\left(A_C(x) \right)_i = x_i - \sum_{j=1}^{d} c_{ij} \lfloor x_i - x_j \rceil \quad \text{mod } 1, \tag{3}$$

for $i = 1, 2, \ldots, d$. Note that the P_{ij} are (flat) co-dimension one submanifolds of $\mathbb{T}^d$ which may intersect in a complicated way. Notice also that the diagonal entries of C do not have any bearing on (3), since $\lfloor x_i - x_j \rceil = 0$ if $i = j$.

Remark. We can rewrite (3) as

$$\left(A_C(x) \right)_i = R_{c_{i1} \lfloor x_1 - x_i \rceil} \circ R_{c_{i2} \lfloor x_2 - x_i \rceil} \circ \ldots \circ R_{c_{id} \lfloor x_d - x_i \rceil}(x_i),$$

where $R_\rho : \mathbb{S}^1 \to \mathbb{S}^1$ denotes the counterclockwise rotation by angle $2\pi\rho$. The rotation map $R_{c_{ij} \lfloor x_j - x_i \rceil}$ can be intuitively thought of as the "influence" or "force" of site j over site i. Notice that any two of these maps commute. This representation shows that the nature of the averaging map defined by equation (3) is truly that of a pairwise spatial interaction.

We now come to the analog of the condition $\alpha < 1/2$ in the two dimensional case. Away from the set $P(C)$, the derivative of A_C, denoted DA_C, is constant. To make this statement precise, we identify the tangent spaces at every $x \in \mathbb{T}^d$ with $\mathbb{R}^d$ in the canonical way. It is easy to check from (3) that with respect to this identification and the usual basis of $\mathbb{R}^d$, the matrix representation of DA_C at every $x \in \mathbb{T}^d \setminus P(C)$ is in fact given by C itself. Here the condition that is consistent with A_C having the properties of a diffusion process is to require that DA_C, or C, be positive definite.‖ This condition is discussed in more detail in the next subsection.

We finish by noting that as in the two-dimensional case, the singularity set of the coupled map $\Phi = A_C \circ F$ here is $S = F^{-1}P(C)$, i.e., we have $\Phi : \mathbb{T}^d \setminus S \to \mathbb{T}^d$.

2.3. Positivity and spectral properties of $DA_C \equiv C$

As mentioned in the previous subsection, it makes physical sense to assume that DA_C be positive definite. The main point of this subsection, Proposition 2.4, describes the spectral properties of $DA_C \equiv C$ under this natural hypothesis. We start with some necessary and sufficient conditions for positivity.

Lemma 2.1. *Let C be a $d \times d$ coupling matrix, and let V be the diagonal matrix defined by $(V)_{ii} = v_i = \sum_{j \neq i} c_{ij}$, $i = 1, \ldots, d$. If $\bar{v} = \max_i v_i \leqslant 1/2$, then DA_C is positive semi-definite. If the inequality is strict, then DA_C is positive definite.*

Proof. Let I be the $d \times d$ identity matrix. The matrices $I - C$ and $2V$ are symmetric and (non-strictly) diagonally dominant; therefore they are positive semi-definite. (A matrix (a_{ij}) is said to be *diagonally dominant* if the absolute value of the diagonal entry a_{ii} is greater than or equal to the sum of the absolute values of the other entries in each row, and if the same holds for the columns.) Their largest eigenvalues are $\|I - C\|$ and $\|2V\|$ respectively. The matrix $2V - (I - C)$ is also diagonally dominant, hence also positive semi-definite. By [26] (Theorem 16, page 132), $\|I - C\| \leqslant \|2V\| = 2\bar{v}$.

Each eigenvector of C with eigenvalue λ_i is of course an eigenvector of $I - C$ with eigenvalue $1 - \lambda_i$. Hence the least eigenvalue of C is equal to $1 - \|I - C\| \geqslant 1 - 2\bar{v}$, which is non-negative if $\bar{v} \leqslant 1/2$, and positive if $\bar{v} < 1/2$. □

Another sufficient condition for positivity is

Lemma 2.2. *Let C be a $d \times d$ coupling matrix. If $\bar{c} = \max_{i \neq j} c_{ij} \leqslant 1/d$, then DA_C is positive semi-definite. If the inequality is strict, then DA_C is positive definite.*

The proof is postponed to subsection 3.2, where it fits more naturally, since this lemma is motivated by the discussion there.

Lemma 2.3. *Let $\bar{v}$ be as in lemma 2.1, and $\bar{c}$ be as in lemma 2.2. If $\bar{v} \geqslant 1$ or if $\bar{c} \geqslant 1/2$, then DA_C is not positive definite.*

Proof. Suppose first that $\bar{v} \geqslant 1$. Without loss of generality, we may assume that $v_1 \geqslant 1$. Let $w = (1, 0, \ldots, 0)^T \in \mathbb{R}^d$. Then the first entry of $DA_C \cdot w = Cw$ is not positive, hence $w^T DA_C w \leqslant 0$. Now suppose that $\bar{c} \geqslant 1/2$. Once again, we may assume without loss of generality that $c_{12} \geqslant 1$. If $z = (1, -1, 0, \ldots, 0)^T \in \mathbb{R}^d$, then $z^T DA_C z \leqslant 0$. □

‖ This is physically the most interesting case. Even though we discuss explicitly only this case, many of the results in this paper continue to hold, with slight modifications, without this positivity condition.

The following result is central to our discussion:

Proposition 2.4. *Let C be a $d \times d$ positive definite coupling matrix. Then the eigenvalues λ_i of DA_C satisfy*

$$1 = \lambda_1 > \lambda_2 \geqslant \lambda_3 \geqslant \cdots \geqslant \lambda_d > 0. \tag{4}$$

Moreover, DA_C admits an orthonormal basis of eigenvectors $\{z_i\}$ corresponding to the λ_i, and the eigenvector z_1 is a multiple of $(1, 1, \ldots, 1)^T \in \mathbb{R}^d$.

Proof. From the symmetry of C it follows that the λ_i are real and that C admits an orthonormal basis of eigenvectors. The λ_i are positive since C is assumed to be strictly positive definite. The eigenvalues of $I - C$ are $\eta_1 = 1 - \lambda_i$. But $I - C$ is positive semi-definite (see the proof of lemma 2.1), so $\eta_i \geqslant 0$, and thus $\lambda_i \leqslant 1$. By our definition of c_{ii}, the entries on each row of $I - C$ add up to zero. Therefore $(1, 1, \ldots, 1)^T \in \mathbb{R}^d$ is an eigenvector of $I - C$ with eigenvalue $\eta_1 = 0$, equivalently $\lambda_1 = 1$.

It remains to show that the eigenspace corresponding to eigenvalue λ_1 is one-dimensional. By lemma 2.3, $\bar{v} < 1$ (where $\bar{v}$ is as in lemma 2.1), so the entries of C are non-negative. The diagonal entries, in particular, are positive. With these facts, it is easy to see that C is irreducible and aperiodic, i.e., there is $n \in \mathbb{N}$ such that all entries in C^n are strictly positive. (This step uses the fact that G is connected.) Hence the Perron-Frobenius Theorem applies to C to give the desired result. □

3. Simplest examples

In this section we consider some situations for which technical estimates are kept to a minimum, namely where the f_i are linear and coupling constants are equal. The coupling matrix C is assumed throughout to be positive definite.

3.1. Linear local maps, equal coupling strengths

We assume all the local maps are identical and linear, i.e., we fix $k \in \mathbb{Z}^+$ and $b \in \mathbb{R}$, and for all i, let $f_i : \mathbb{S}^1 \to \mathbb{S}^1$ be given by $f_i(x) = kx + b \mod 1$. (For $k \geqslant 2$, the system is equivalent one in which $b = 0$ by a linear change of coordinates.) In this linear case, $D\Phi \equiv kDA_C$; hence it has the same eigenspaces as DA_C and eigenvalues

$$k = \mu_1 > \mu_2 \geqslant \mu_3 \geqslant \cdots \geqslant \mu_d > 0 \tag{5}$$

where $\mu_i = k\lambda_i$, $\{\lambda_i\}$ being the eigenvalues of DA_C (see Proposition 2.4).

We will also restrict our attention to coupling graphs in which all edges are assigned equal coupling strengths, which we denote by α. This provides a framework in which to study the dependence of the spectrum of $D\Phi_\alpha$ upon the single parameter α, while keeping the graph fixed.

In this special case, the following notation is convenient: Let $\tilde{C}$ be the incidence matrix, i.e., $\tilde{c}_{ij} = 1$ if $(i, j) \in \mathcal{E}$, $\tilde{c}_{ij} = 0$ otherwise, and let $\tilde{V}$ be the diagonal matrix with $\tilde{v}_{ii} = \sum_{j \neq i} \tilde{c}_{ij}$ (the valence of vertex i of G). In this notation, the coupling matrix C introduced earlier is given by $C = I - \alpha(\tilde{V} - \tilde{C})$, and if we denote the spectrum of $\tilde{V} - \tilde{C}$ by $\{\tilde{\eta}_j\}$, with the $\tilde{\eta}_j$ ordered from smallest to largest, then the eigenvalues of $D\Phi$ are given by

$$\mu_j = k\lambda_j = k(1 - \alpha\tilde{\eta}_j), \qquad \text{for } j = 1, 2, \ldots, d; \tag{6}$$

in particular, $\tilde{\eta}_1 = 0$ and has multiplicity one.

The following facts follow immediately from (6): When α is small, all of the μ_j are close to k. Thus for $k \geqslant 2$, Φ is expanding, more accurately *piecewise expanding* (since there is a discontinuity set S) for small α. Figure 3(a) illustrates a possible example of the positions of the μ_j for $k \geqslant 2$. As α increases, μ_1 remains fixed at k, while the other eigenvalues decrease (figure 3(b)). At some critical value of α, the smallest eigenvalue of $D\Phi$ reaches 1; at this point Φ ceases to be expanding. As α increases further, unstable eigenspaces switch to stable spaces, as their corresponding eigenvalues move from the right to the left of 1 (figure 3(c)). It is important to note that while the eigenvalues μ_j vary with α, the associated eigenspaces do not. These eigenspaces are the same as those of $\tilde{V} - \tilde{C}$, which is a fixed linear map. In figure 3(d), all but one of the eigenspaces of $D\Phi$ have become contracting under $D\Phi$. This does not always happen, however: As we increase α, there is a value $\alpha_{\max}$ at which μ_d, the smallest eigenvalue of $D\Phi$, reaches zero. Beyond that point, DA_C ceases to be positive definite. Lemmas 2.1 and 2.2 provide lower bounds on $\alpha_{\max}$.
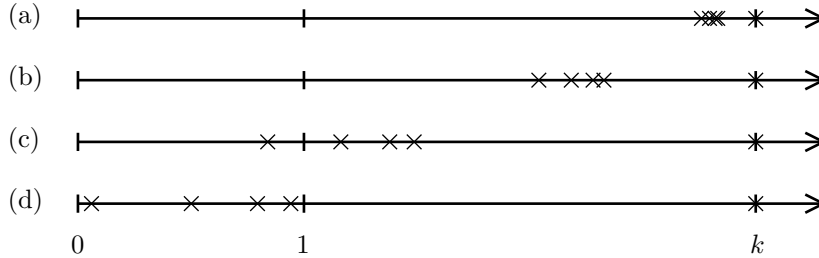
**Figure 3.** The eigenvalues μ_j (marked by $\times$'s) move left as α increases.

Nonlinear versions of the results above are discussed in Section 4.

3.2. Concrete examples

We compute here explicitly the eigenvalues for a few specific coupling graphs. All coupling strengths are equal to α in the examples below. The *distinct* eigenvalues of $D\Phi$ are denoted by $\{\bar{\mu}_j\}$.

3.2.1. Complete graph, or all-to-all coupling. As a first example, we consider the complete graph with d vertices, i.e., $\Omega = \{1, \ldots, d\}$ and $(i,j) \in \mathcal{E}$ for all $i, j \in \Omega$, $i \neq j$.
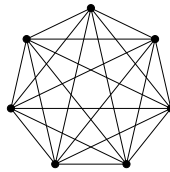
Figure 4. All-to-all (complete) coupling graph for $d = 7$.

Claim. $D\Phi = kDA_C$ *has exactly two eigenvalues,* $\bar{\mu}_1 = k$, *with multiplicity 1, and* $\bar{\mu}_2 = k(1 - \alpha d)$, *with multiplicity* $d - 1$.

Consider for definiteness the expanding case, i.e., $k \geqslant 2$. The assertion above implies that as we increase α from zero, some "phase transitions" occur: Initially, Φ is piecewise expanding in all directions. At $\alpha = (k-1)/kd$, a codimension one subspace switches from unstable to stable. At $\alpha = 1/d$, all but one of the eigenvalues become 0.

It is natural to wonder (for any k) what the eventual dynamics will be in the case of a strong enough coupling. One possibility is synchronization, and for $d = 2$, an easy exercise shows that for any $\alpha > (k-1)/2k$, regardless of initial condition the system will eventually synchronize, i.e., the trajectory will tend to the diagonal. It may be tempting to think that in the case of strong enough all-to-all coupling in any dimension, synchronization is also inevitable independent of initial condition, *but that is not true!* See Section 5.3 for a detailed analysis of the case $d = 3$.

To prove the claim above, recall that $C = I - \alpha(\tilde{V} - \tilde{C})$, where in this case

$$
\tilde{C} = \begin{pmatrix} 0 & 1 & 1 & \cdots & 1 \\ 1 & 0 & 1 & \cdots & 1 \\ 1 & 1 & 0 & \cdots & 1 \\ \vdots & \vdots & \vdots & \ddots & \vdots \\ 1 & 1 & 1 & \cdots & 0 \end{pmatrix} \quad \text{and} \quad \tilde{V} = \begin{pmatrix} d-1 & 0 & \cdots & 0 \\ 0 & d-1 & \cdots & 0 \\ \vdots & \vdots & \ddots & \vdots \\ 0 & 0 & \cdots & d-1 \end{pmatrix}. \tag{7}
$$

The eigenvalues of $\tilde{V} - \tilde{C}$ are 0 (with multiplicity 1) and d (with multiplicity $d-1$). To prove this statement, let J be the $d \times d$ matrix

$$
J = \begin{pmatrix} 0 & & & & 1 \\ 1 & 0 & & & \\ & 1 & 0 & & \\ & & \ddots & \ddots & \\ & & & 1 & 0 \end{pmatrix} \tag{8}
$$

(where empty spaces represent zeros). Then $\tilde{V} - \tilde{C} = (d-1)I - J - J^2 - J^3 - \ldots - J^{d-1}$. The eigenvalues of J are the d-th roots of unity $\xi_j = e^{2\pi i(j-1)/d}$, $j = 1, 2, \ldots, d$, hence the eigenvalues of $\tilde{V} - \tilde{C}$ are $d - 1 - \sum_{k=1}^{d-1} \xi_j^k$, which is equal to zero if $j = 1$ and equal to d otherwise. The assertion on the eigenvalues of $D\Phi$ follows.

One sees in the example above that DA_C is positive definite if and only if $\alpha < 1/d$. This is what motivates Lemma 2.2, the proof of which we now give. But first we need the following general lemma (which applies to *all* coupling matrices).

Lemma 3.1. *Let C_1 and C_2 be arbitrary $d \times d$ coupling matrices, let A_{C_1} and A_{C_2} be the associated coupling maps, and λ_i^1 and λ_i^2 the eigenvalues of DA_{C_1} and DA_{C_2} respectively. We list the λ_i^ℓ with multiplicity and in decreasing order, i.e., $\lambda_1^\ell \geqslant \lambda_2^\ell \geqslant \cdots \geqslant \lambda_d^\ell$, $\ell = 1, 2$. If $(C_1)_{ij} \geqslant (C_2)_{ij}$ for all $i \neq j$, then $\lambda_i^1 \leqslant \lambda_i^2$, for $i = 1, 2, \ldots, d$.*

Proof. The argument is similar to that of lemma 2.1. We denote the eigenvalues of $I - C_\ell$ by η_i^ℓ, arranged in *increasing* order. The symmetric matrix $(I - C_1) - (I - C_2) = C_2 - C_1$ is (non-strictly) diagonally dominant with non-negative diagonal entries, hence it is positive semi-definite. Once again, it follows immediately from [26] (theorem 16, page 132) that $\eta_i^1 \geqslant \eta_i^2$, for $i = 1, 2, \ldots, d$. Since the eigenvalues of $DA_{C_\ell} = C_\ell$ are $\lambda_i^\ell = 1 - \eta_i^\ell$, we have $\lambda_i^1 \leqslant \lambda_i^2$. $\square$

Lemma 3.1 validates the intuition that stronger couplings lead to more contraction in DA_C (the eigenvalues λ_i decrease). Given a maximum coupling strength $\bar{c}$, the "most contractive" coupling matrix is, therefore, the complete graph with all coupling strengths exactly equal to the maximum $\bar{c}$. This idea is used in the following proof.

Proof of lemma 2.2. Let C_1 be the $d \times d$ coupling matrix defined by $C_1 = I - \bar{c}(\tilde{V} - \tilde{C})$, where $\tilde{V}$ and $\tilde{C}$ are as in (7), i.e., C_1 is the coupling matrix associated with all-to-all coupling with strength $\bar{c}$. Then $(C_1)_{ij} \geqslant (C)_{ij}$ for $i \neq j$, so Lemma 3.1 implies that the smallest eigenvalue of DA_C is greater than or equal to the smallest eigenvalue of DA_{C_1}, which is $1 - \bar{c}d$ (see the proof of the claim above). Since $\bar{c} \leqslant 1/d$, DA_C is positive semi-definite, and positive definite if the inequality is strict. $\square$

3.2.2. Cycle. Our second example is when the coupling graph is a loop with d vertices, labeled counter-clockwise for definiteness. The eigenvalues of $D\Phi$ in this
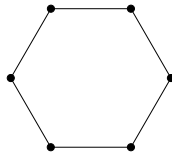
Figure 5. Cycle coupling graph for $d = 6$.

case are $\mu_j = k - 2k\alpha\big(1 - \cos(2\pi(j-1)/d)\big)$, $j = 1, \ldots, d$ (warning: written in this form, the μ_j are not ordered as in (5)). This is shown by the same method used in the previous example; observe that in the present case we have $\tilde{V} - \tilde{C} = 2I - J - J^{d-1}$, where J is as in (8).

The eigenspaces of $D\Phi$ can be described as follows. If U is the $d \times d$ matrix given by $(U)_{(i+1),(j+1)} = \cos(2\pi ij/d) + \sin(2\pi i(d-j)/d)$, for $i, j = 0, 1, \ldots, d-1$, then the j-th column of U is an eigenvector of DA_C corresponding to the eigenvalue μ_j. (It is easy to see that U has full rank, its columns being orthogonal).

The eigenvectors of $D\Phi$ are thus simply (discrete) sinusoids. The sinusoidal eigenvectors of higher frequencies correspond to smaller eigenvalues, and therefore expand less (or contract more) than eigenvectors of lower frequency. This fits nicely with our understanding of A_C as a discrete diffusion or heat process. Indeed, the eigenvalues and eigenvectors we obtain in this case are exactly those of the discrete heat equation on a uniform circle (with uniform grid).

Finally, recall that for all coupling matrices, the most expanded direction is $y_1 = (1, 1, 1, \ldots, 1)^T$. Thus in the case $k \geqslant 2$, perturbing *any* configuration $(x_1, \ldots, x_d) \in \mathbb{S}^1 \times \ldots \times \mathbb{S}^1$ by adding (the same) δ to each coordinate is the fastest way to get the two Φ-orbits to diverge. By the same token, perturbations that result in the slowest divergence are those in the least expanded direction. In the case of a loop with an even number of vertices, $y_d = (1, -1, 1, \ldots, -1)^T$, which makes intuitive sense, for the alternating pattern maximizes the averaging effects of A_C.

Examples in which piecewise expanding interval maps are coupled along cyclic graphs were studied in [22], with results similar to ours.

3.2.3. Path. Not surprisingly, the "chain" or "path" (as in Figure 6) is very similar to the previous example. The eigenvalues of $D\Phi$ are $\mu_j = k - 2k\alpha\big(1 - \cos(\pi(j-1)/d)\big)$,

Figure 6. Path coupling graph for $d = 6$.

$j = 1, \ldots, d$, and the associated eigenvectors are the columns of the matrix given by $(U)_{(i+1),(j+1)} = \cos(\pi(1/2+i)j/d)$, for $i, j = 0, \ldots, d-1$. The same remarks as in the previous case apply.

3.2.4. Complete bipartite graph. The final example is rather interesting, in that it gives further insight into the relationship between coupling and contraction. We consider complete bipartite graphs, which for definiteness we assume to have an even number of vertices with exactly half in each of the two groups (as in Figure 7). The
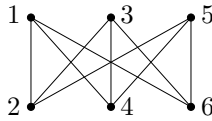

Figure 7. Complete bipartite coupling graph for $d = 6$.

eigenvalues of $D\Phi$ are $\bar\mu_1 = k$, $\bar\mu_2 = k - k\alpha d/2$ (with multiplicity $d-2$), and $\bar\mu_3 = k - k\alpha d$. As before, this is proved by showing that $\hat V - \tilde C = \frac{d}{2}I - J - J^3 - \ldots - J^{d-3} - J^{d-1}$ where J is as in (8) and the vertices are labeled as in Figure 7. The eigenvectors corresponding to $\bar\mu_1$ and $\bar\mu_3$ are $y_1 = (1, 1, \ldots, 1)^T$ and $y_3 = (1, -1, 1, \ldots, -1)^T$ respectively. Intuitively, y_3 is the natural candidate for the direction with the strongest contraction, for it maximizes the averaging effects of A_C.

From Lemma 3.1, we see that for a given coupling strength, the more edges a graph has, the stronger the contraction. It follows that the strongest contraction occurs in the all-to-all case. But notice that $k(1 - \alpha d)$, the smaller of the two eigenvalues in the all-to-all example, is also an eigenvalue for the complete bipartite graph. In other words, adding edges with coupling strength $\leqslant \alpha$ connecting vertices within each of the two groups will not produce a stronger maximum contraction. (One way to see this is via the following small computation, details of which we leave to the reader: consider the case $d = 3$ and $\alpha < 1/3$, and notice that the strongest contraction remains unchanged as one goes from the path to the triangle.)

4. Robust hyperbolicity of the non-linear coupled map

Given the spectral properties of $D\Phi$ when the local maps are all equal to some $f(x) = kx + b \bmod 1$, it is to be expected that Φ will retain some form of hyperbolic behavior when the f_i are not too far from linear. In this section, we make precise these ideas with estimates.

Setting for this section. We assume that the local maps $f_i : \mathbb{S}^1 \to \mathbb{S}^1$, $i = 1, \ldots, d$, are of the form $f_i = f + \varepsilon g_i + b_i \bmod 1$ where $f(x) = kx \bmod 1$ for some positive integer k, the g_i are C^1 maps of degree zero on the circle with $|g_i'| \leqslant 1$, and $b_i \in \mathbb{R}$. If ε is small enough, then the f_i are orientation-preserving local diffeomorphisms of degree k. Aside from being positive definite, no other conditions are imposed on the coupling matrix C, and $\Phi = A_C \circ F$ as before.

Our main results are Propositions 4.1 and 4.2, which establish the existence of filtrations of invariant "stable" and "unstable" subbundles when ε is small enough. These propositions lead immediately to invariant splittings of various kinds; the results are summarized in Theorem 4.4.

4.1. "Stable" and "unstable" filtrations

We denote the *distinct* eigenvalues of DA_C by

$$1 = \bar{\lambda}_1 > \bar{\lambda}_2 > \bar{\lambda}_3 > \ldots > \bar{\lambda}_r > 0,$$

and the eigenspace corresponding to $\bar{\lambda}_i$ by V_i. Since our goal in this section is to construct subbundles invariant under $D\Phi = DA_C \cdot DF$ when DF is uniformly close to the homothetic map kI, it is natural to work in coordinates compatible with the spaces V_i.

For each fixed $\ell \in \{1, 2, \ldots, r-1\}$, we define $V^+ = V_\ell^+$ and $V^- = V_\ell^-$ by

$$V^+ = \bigoplus_{i=1}^{\ell-1} V_i \qquad \text{and} \qquad V^- = \bigoplus_{i=\ell}^{r} V_i, \tag{9}$$

and let $\|\cdot\|^\vee$ be the maximum norm with respect to $V^+ \oplus V^-$, that is, for $w = (u, v) \in V^+ \oplus V^-$, we have $\|w\|^\vee = \max\{\|u\|, \|v\|\}$, where $\|\cdot\|$ represents the Euclidean norm in both V^+ and V^-.

Identifying the tangent bundle over $\mathbb{T}^d$ with $\mathbb{T}^d \times \mathbb{R}^d$, we observe that $\mathbb{T}^d \times V^+$ and $\mathbb{T}^d \times V^-$ are DA_C-invariant subbundles. Our first result gives conditions for the existence of a $D\Phi$-invariant subbundle E_ℓ^- corresponding to $\mathbb{T}^d \times V^-$. Since our construction involves infinite forward orbits of Φ, E_ℓ^- (if it exists) will be a subbundle of $Y^+ \times \mathbb{R}^d$ where $Y^+ = \mathbb{T}^d \setminus S_\infty$ and $S_\infty = \bigcup_{n=0}^\infty \Phi^{-n}(S)$. It is easy to check that $\Phi^{-1}(Y^+) = Y^+$ and $\Phi(Y^+) \subset Y^+$. The fiber of E_ℓ^- over $x \in Y^+$ is denoted $E_\ell^-(x)$.

Recall the meanings of k and ε at the beginning of this section.

Proposition 4.1 (Existence of "stable" subbundles). *If $\varepsilon < k(\bar{\lambda}_{\ell-1} - \bar{\lambda}_\ell)/4$, then $Y^+ \times \mathbb{R}^d$ admits a Borel-measurable subbundle E_ℓ^- with the following properties:*

(i) *E_ℓ^- is $D\Phi$-invariant, that is, $D\Phi(x) \cdot E_\ell^-(x) = E_\ell^-\big(\Phi(x)\big)$.*

(ii) *$\dim E_\ell^-(x) = \dim V^-$.*

(iii) *If $w \in E_\ell^-(x)$, then $\left\|D\Phi(x) \cdot w\right\|^\vee \leqslant (k\bar{\lambda}_\ell + 2\varepsilon) \left\|w\right\|^\vee$.*

This proposition is proved in Section 4.3. As usual, the proof uses the idea of invariant cones. Define the *negative cone* with respect to the splitting $V^+ \oplus V^-$ to be $C^- = \{ (u, v) \in V^+ \oplus V^- ; \|u\| \leqslant \|v\| \}$. We say C^- is $(D\Phi)^{-1}$-*invariant* if for every $x \in X$, $\big(D\Phi(x)\big)^{-1} C^- \subset C^-$. We show in Section 4.3 that C^- is $D\Phi^{-1}$-invariant; in fact, we show that it is *strictly uniformly* $(D\Phi)^{-1}$-invariant, meaning there exists $\delta > 0$ such that for all $x \in Y^+$, the distance between $\big(D\Phi(x)\big)^{-1} C^-$ and ∂C^-, the boundary of C^-, is at least δ. See Section 4.3 for more detail.

The fiber $E_\ell^-(x)$ at $x = x_0 \in Y^+$ is constructed as follows: If $x_n = \Phi^n(x)$ for $n \in \mathbb{N}$, then

$$E_\ell^-(x) = \bigcap_{n=0}^\infty \big(D\Phi(x_0)\big)^{-1} \circ \big(D\Phi(x_1)\big)^{-1} \circ \cdots \circ \big(D\Phi(x_n)\big)^{-1} C^-.$$

Remark. In the proposition, we have referred to the subbundle E_ℓ^- as "stable" even though vectors in it are not necessarily contracted under $D\Phi$. Their rates of expansion, however, are bounded above by $k\bar\lambda_\ell + 2\varepsilon$. As we will see, vectors outside of E_ℓ^- will have a strictly larger asymptotic growth rate in a sense to be made precise.

The next proposition is completely analogous to Proposition 4.1, except that it deals with the construction of "unstable", rather than "stable", subbundles. This means that we need infinitely long *backward* orbits of Φ. Since Φ is not necessarily onto, not all points have inverse images, so we restrict to the set of points that do. In addition, if $k \geqslant 2$, then Φ is not one-to-one, and it is necessary to work with its natural extension. We recall the basic idea (see [29]).

We first specify the the subset $Y \subset Y^+$ of points that have at least one infinite backward orbit, that is, $Y = \bigcap_{n=0}^\infty \Phi^n(Y^+)$. It is easy to check that $\Phi(Y) = Y$ and $\Phi^{-1}(Y) = Y$. The *natural extension* of $\Phi : Y \to Y$ is the dynamical system $\hat\Phi : \hat Y \to \hat Y$ where $\hat Y$ is the set of histories of $x \in Y$ and $\hat\Phi$ is the time shift. More precisely,

$$\hat Y = \left\{ \boldsymbol{x} = (\ldots, x_{-1}, x_0) \; ; \; x_n \in Y \text{ and } \Phi(x_{n-1}) = x_n \text{ for all } n \in \mathbb{Z}^- \right\} \tag{10}$$

and

$$\hat\Phi(\ldots, x_{-1}, x_0) = \big(\ldots, x_{-1}, x_0, \Phi(x_0)\big). \tag{11}$$

Then $\hat\Phi$ is invertible and there is a natural projection $\pi : \hat Y \to Y$ with $\pi(\ldots, x_{-1}, x_0) = x_0$. For $\boldsymbol{x} \in \hat Y$ and $n \in \mathbb{Z}^+$, we *define* $D\hat\Phi^n(\boldsymbol{x}) : \mathbb{R}^d \to \mathbb{R}^d$ to be the linear map

$$D\Phi\big(\pi(\hat\Phi^{n-1}(\boldsymbol{x}))\big) D\Phi\big(\pi(\hat\Phi^{n-2}(\boldsymbol{x}))\big) \cdots D\Phi\big(\pi(\Phi(\boldsymbol{x}))\big) D\Phi\big(\pi(\boldsymbol{x})\big),$$

and $D\hat\Phi^{-n}(\boldsymbol{x}) : \mathbb{R}^d \to \mathbb{R}^d$ to be $\big(D\hat\Phi^n(\hat\Phi^{-n}(\boldsymbol{x}))\big)^{-1}$.

Proposition 4.2 (Existence of "unstable" subbundles). *If $\varepsilon < k(\bar\lambda_{\ell-1} - \bar\lambda_\ell)/4$, then $\hat Y \times \mathbb{R}^d$ admits a Borel-measurable subbundle $E_{\ell-1}^+$ with the following properties:*

(i) $E_{\ell-1}^+$ is $D\hat\Phi$-invariant, that is, $D\hat\Phi(\boldsymbol{x}) \cdot E_{\ell-1}^+(\boldsymbol{x}) = E_{\ell-1}^+\big(\hat\Phi(\boldsymbol{x})\big)$.

(ii) $\dim E_{\ell-1}^+(\boldsymbol{x}) = \dim V^+$.

(iii) If $w \in E_{\ell-1}^+(\boldsymbol{x})$, then $\big\| D\hat\Phi(\boldsymbol{x}) \cdot w \big\|^\vee \geqslant (k\bar\lambda_{\ell-1} - 2\varepsilon) \|w\|^\vee$.

The proof is given in Section 4.3. The fiber $E_{\ell-1}^+(\boldsymbol{x})$ at $\boldsymbol{x} = (\ldots, x_{-2}, x_{-1}, x_0) \in \hat Y$ is given by

$$E_{\ell-1}^+(\boldsymbol{x}) = \bigcap_{n=1}^\infty D\Phi(x_{-1}) \circ D\Phi(x_{-2}) \circ \cdots \circ D\Phi(x_{-n}) C^+,$$

where $C^+ = \{ (u, v) \in V^+ \oplus V^- \; ; \; \|u\| \geqslant \|v\| \}$ is the *positive cone* with respect to the splitting $V^+ \oplus V^-$, and we show that C^+ is strictly uniformly invariant under $D\Phi$. As explained earlier, vectors in $E_{\ell-1}^+$ are not necessarily expanded under $D\Phi$ (or contracted under backward iterations), only more so than vectors not in this subbundle.

4.2. Invariant splittings

Abusing notation slightly, we use E_ℓ^- to denote also the corresponding stable subbundle of $\hat Y \times \mathbb{R}^d$. Taking intersections of E_ℓ^+ and E_ℓ^- for different values of ℓ, we construct in this subsection a set of invariant subbundles; the expansion or contraction rates of $D\Phi$ in each one lie within specified intervals. Our main result is summarized in Theorem 4.4. First we give a special case. Recall once again the meanings of $\bar\lambda_i$, k and ε at the beginning of the section.

Proposition 4.3 (Hyperbolic splitting). *If there is an ℓ with*

$$k\bar\lambda_\ell + 2\varepsilon < 1 < k\bar\lambda_{\ell-1} - 2\varepsilon, \tag{12}$$

then $\hat\Phi : \hat Y \to \hat Y$ is hyperbolic. More precisely, $\hat Y \times \mathbb{R}^d = E^u \oplus E^s$ where $E^s = E_\ell^-$ and $E^u = E_{\ell-1}^+$ are the subbundles given by Propositions 4.1 and 4.2 respectively. As the notation suggests, vectors in E^u uniformly expand and vectors in E^s uniformly contract under $D\hat\Phi$.

This follows directly from the propositions. Note that the inequalities in (12) are *strict*, so that (i) the angles between vectors in E^u and E^s are uniformly bounded away from zero (recall that $\boldsymbol{x} \mapsto E_{\ell-1}^+(\boldsymbol{x}), E_\ell^-(\boldsymbol{x})$ need not be continuous if Φ is only piecewise smooth), and (ii) there is some δ_0 such that $\left\|D\hat\Phi(\boldsymbol{x}) \cdot w\right\|^\vee \geqslant (1 + \delta_0) \left\|w\right\|^\vee$ if $w \in E_{\ell-1}^+(\boldsymbol{x})$, and $\left\|D\hat\Phi(\boldsymbol{x}) \cdot w\right\|^\vee \leqslant (1 - \delta_0) \left\|w\right\|^\vee$ if $w \in E_{\ell-1}^-(x_0)$, where the norm here is the same as that of Propositions 4.1 and 4.2, i.e., it is the maximum norm with respect to $V_\ell^+ \oplus V_\ell^- = V^+ \oplus V^-$.

To state the general case, we need some terminology:

Definition. Let $\mathcal{A} = \{a_1, a_2, \ldots, a_n\}$ be a finite set of real numbers, and assume they are indexed in decreasing order, i.e. $a_i \geqslant a_{i+1}$. Given $\delta \geqslant 0$, the *δ-bunching* of $\mathcal{A}$ is the partition given by

$$\mathcal{A}_1 = \{a_{i_1} = a_1, a_2, \ldots, a_{i_2-1}\}, \; \mathcal{A}_2 = \{a_{i_2}, \ldots, a_{i_3-1}\}, \; \ldots, \; \mathcal{A}_m = \{a_{i_m}, \ldots, a_n\}$$

where $a_i - a_{i+1} \leqslant \delta$ if a_i and a_{i+1} are in the same $\mathcal{A}_j$, and $a_{i_j} - a_{i_j-1} > \delta$ for $j = 2, 3, \ldots, m$.

Theorem 4.4. *Given C, k and $\varepsilon > 0$, let $\mathcal{A}_1, \ldots, \mathcal{A}_m$ be the $(4\varepsilon/k)$-bunching of the $\{\bar\lambda_i\}$, and let Φ be as in the setting for this section. Then there exists a $D\hat\Phi$-invariant Borel-measurable decomposition*

$$\hat Y \times \mathbb{R}^d = L_1 \oplus \ldots \oplus L_m \tag{13}$$

and a constant $c > 0$ such that for every $j \in \{1, \ldots, m\}$, $n \in \mathbb{Z}$, $\boldsymbol{x} \in \hat Y$ and $w \in L_j(\boldsymbol{x})$ with $w \neq 0$, we have

$$\frac{1}{c}\big(k\underline\sigma_j - 2\varepsilon\big)^n \leqslant \frac{\left\|D\hat\Phi^n(\boldsymbol{x}) \cdot w\right\|}{\|w\|} \leqslant c\big(k\bar\sigma_j + 2\varepsilon\big)^n \tag{14}$$

where $\underline\sigma_j$ and $\bar\sigma_j$ denote, respectively, the smallest and greatest elements of $\mathcal{A}_j$.

The norm used in (14) is the usual Euclidean norm. This theorem also follows directly from Propositions 4.1 and 4.2. In fact, for $\boldsymbol{x} = (\ldots, x_{-1}, x_0) \in \hat Y$, the space $L_j(\boldsymbol{x})$ is given by $E_{i_{j+1}-1}^+(\boldsymbol{x}) \cap E_{i_j}^-(x_0)$.

Remarks. Let both the hypotheses and notation be as in Theorem 4.4.

(i) (*Dominated splitting*) Notice that for any j, $1 \leqslant j < m$, if we let $L^+ = \bigoplus_{i \leqslant j} L_i$ and $L^- = \bigoplus_{i > j} L_i$, then the splitting $L^+ \oplus L^-$ satisfies a *domination condition* (see e.g. [17], Chapter 4): (i) angles between vectors in L^+ and L^- are uniformly separated, and (ii) growth rates of vectors in L^+ are strictly higher than those in L^-, since there is a $\delta_0 > 0$ such that $k\underline\sigma_j - 2\varepsilon \geqslant k\bar\sigma_{j+1} + 2\varepsilon + \delta_0$. Notice that we have used the term here in a slightly more general setting than usual, namely for maps that are piecewise smooth and not necessary one-to-one.

(ii) (*Partial hyperbolicity*) Supposing there exist j, j', $1 \leqslant j < j' \leqslant m$, such that $k\underline{\sigma}_j - 2\varepsilon > 1 > k\bar{\sigma}_{j'} + 2\varepsilon$, we let $E^u = \bigoplus_{1 \leqslant i \leqslant j} L_i$, $E^c = \bigoplus_{j < i < j'} L_i$ and $E^s = \bigoplus_{i \geqslant j'} L_i$. If $E^c = \{0\}$, then $E^u \oplus E^s$ is the uniform hyperbolic splitting of Proposition 4.3. If $E^c \neq \{0\}$, then we may view $E^u \oplus E^c \oplus E^s$ as a *partially hyperbolic* splitting of $\hat{Y} \times \mathbb{R}^d$ (see e.g. [17], Chapter 1). As above, we have used the term here in a slightly more general setting than usual.

(iii) Finally, we remark that while the subbundles L_j depend on the choice of g_i, the number of factors in the splitting (13) and the bounds in (14) depend only on C, k and ε.

It is interesting to visualize how the local dynamics of Φ change with ε. For $\varepsilon = 0$, Φ is piecewise linear, so the subbundles L_j in (13) are simply the eigenspaces of DA_C, and the rates of expansion or contraction in each L_j are the eigenvalues $\bar{\mu}_j = k\bar{\lambda}_j$ of $D\Phi$. This is illustrated in Figure 8(a). When $\varepsilon > 0$, the directions of L_j may vary from point to point, as may the expansion and contraction rates within each L_j, but as long as ε is small enough, the splitting in the $\varepsilon = 0$ case persists (Figure 8(b)). As ε increases, some of the previously invariant subbundles may "coalesce" into higher-dimensional invariant subbundles, as illustrated in Figures 8(c),(d).
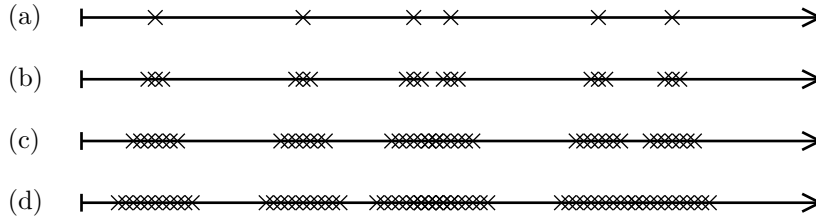
Figure 8. Illustration of the process by which the invariant sub-bundles L_ℓ "coalesce". The parameter ε increases from (a) to (d).

4.3. Proofs of propositions 4.1 and 4.2

Suppose once again that the eigenvalues λ_i of DA_C are written in decreasing order, and let $\{z_i\}$ be a basis of orthonormal eigenvectors, with z_i associated to λ_i.

In this subsection, $D\Phi$, DA_C, and DF will denote the matrix representations of these derivatives with respect to the basis $\{z_i\}$. A diagonal matrix with entries $a_i \in \mathbb{R}$ along the diagonal will be represented by $\operatorname{diag} a_i$ (or, when more precision is required, by $\operatorname{diag}\{a_i \; ; \; i = 1, \ldots, j\}$). Hence we have $DA_C = \operatorname{diag} \lambda_i$, and if we write $DF(x) = kI + \varepsilon G(x)$, we have $G(x) = \mathcal{O}^{-1}\operatorname{diag} g_i'(x_i)\mathcal{O}$, where $\mathcal{O}$ is the orthogonal matrix whose columns are the z_i.

Recall that the positive cone with respect to the splitting $V^+ \oplus V^-$ (see (9)) is given by $C^+ = \{(u,v) \in V^+ \oplus V^- \; ; \; \|u\| \geqslant \|v\|\}$, and the negative cone C^- is defined analogously. We also define $C_\delta^+ = \{(u,v) \in V^+ \oplus V^- \; ; \; \|u\| \geqslant (1+\delta)\|v\|\}$ and $C_\delta^- = \{(u,v) \in V^+ \oplus V^- \; ; \; (1+\delta)\|u\| \leqslant \|v\|\}$, for $\delta > 0$. Note that projectively, the distances between C_δ^+ and ∂C^+ and between C_δ^- and ∂C^- are positive.

Lemma 4.5. *If $\varepsilon < k\left(\bar{\lambda}_{\ell-1} - \bar{\lambda}_\ell\right)/4$, then the positive cone C^+ is strictly uniformly forward invariant and the negative cone C^- is strictly uniformly backward invariant*

under $D\Phi$, that is, there exist δ_1 and $\delta_2 > 0$ such that $D\Phi(x)C^+ \subset C^+_{\delta_1}$ and $\left(D\Phi(x)\right)^{-1}C^- \subset C^-_{\delta_2}$ for any $x \in \mathbb{T}^d \setminus S$.

Proof. Let n be such that span $\{z_1, \ldots, z_n\} = V^+$ and span $\{z_{n+1}, \ldots, z_d\} = V^-$. We write DA_C and G, in block form, as

$$DA_C = \begin{pmatrix} A_1 & 0 \\ 0 & A_2 \end{pmatrix} \quad \text{and} \quad G = \begin{pmatrix} G_{11} & G_{12} \\ G_{21} & G_{22} \end{pmatrix},$$

where $A_1 = \operatorname{diag}\{\lambda_i \ ; \ i = 1, \ldots, n\}$, $A_2 = \operatorname{diag}\{\lambda_i \ ; \ i = n+1, \ldots, d\}$, G_{11} is $n \times n$, G_{12} is $n \times (d-n)$, G_{21} is $(d-n) \times n$ and G_{22} is $(d-n) \times (d-n)$. With this notation,

$$D\Phi = DA_C \cdot DF = k \begin{pmatrix} A_1 & 0 \\ 0 & A_2 \end{pmatrix} + \varepsilon \begin{pmatrix} A_1 G_{11} & A_1 G_{12} \\ A_2 G_{21} & A_2 G_{22} \end{pmatrix}. \quad (15)$$

Now let $(u, v) \in C^+ \subset V^+ \oplus V^-$. Fixing any $x \in \mathbb{T}^d \setminus S$, and letting $(\tilde{u}, \tilde{v}) = D\Phi(x) \cdot (u, v)$, we have

$$\begin{aligned} \|\tilde{u}\| &\geqslant \lambda_n k \|u\| - \varepsilon \|A_1\| \cdot \|G_{11}\| \cdot \|u\| - \varepsilon \|A_1\| \cdot \|G_{12}\| \cdot \|v\| \\ &\geqslant \lambda_n k \|u\| - 2\varepsilon \|u\| \end{aligned} \quad (16)$$

and

$$\begin{aligned} \|\tilde{v}\| &\leqslant \lambda_{n+1} k \|v\| + \varepsilon \lambda_{n+1} \|G_{21}\| \cdot \|u\| + \varepsilon \lambda_{n+1} \|G_{22}\| \cdot \|v\| \quad (17) \\ &\leqslant \lambda_{n+1} k \|u\| + 2\varepsilon \|u\|. \end{aligned} \quad (18)$$

We have used $\|u\| \geqslant \|v\|$ (that is, $(u, v) \in C^+$), $\|A_1\| = 1$, $\|A_2\| = \lambda_{n+1} < 1$, and $\|G_{ij}\| \leqslant 1$. This last fact is not hard to prove. By our choice of n, we have $\bar{\lambda}_{\ell-1} = \lambda_n$ and $\bar{\lambda}_\ell = \lambda_{n+1}$, so from (16) and (18) we get

$$\frac{\|\tilde{u}\|}{\|\tilde{v}\|} \geqslant \frac{\bar{\lambda}_{\ell-1} k - 2\varepsilon}{\bar{\lambda}_\ell k + 2\varepsilon} = a > 1, \quad (19)$$

if $\|u\| > 0$ (otherwise, $(u, v) = (0, 0)$). At this point we set $\delta_1 = a - 1 > 0$.

The assertion that $\left(D\Phi(x)\right)^{-1}C^- \subset C^-_{\delta_2}$ for all $x \in \mathbb{T}^d \setminus S$ follows by similar arguments, but the computations are slightly trickier. We leave them as an exercise. (Hints: $(D\Phi)^{-1}$ can be written as $(k^{-1}I + \varepsilon'H) \cdot (DA_C)^{-1}$, where $\|H\| \leqslant 1$ and $\varepsilon' = k\varepsilon/(k-\varepsilon)$. The value $\delta_2 = \left(k(\bar{\lambda}_{\ell-1} - \bar{\lambda}_\ell) - 4\varepsilon\right)\big/\left(\bar{\lambda}_{\ell-1}\bar{\lambda}_\ell(k\bar{\lambda}_{\ell-1}^{-1} + \varepsilon\lambda_d^{-1})\right)$ works.) $\square$

Lemma 4.6. *Suppose that $\varepsilon < k\left(\bar{\lambda}_{\ell-1} - \bar{\lambda}_\ell\right)/4$. The following statements hold for any $x \in \mathbb{T}^d \setminus S$. If $w \in C^+$, then $\|D\Phi(x) \cdot w\|^\vee \geqslant \left(k\bar{\lambda}_{\ell-1} - 2\varepsilon\right)\|w\|^\vee$. If $w \in \left(D\Phi(x)\right)^{-1}C^-$, then $\|D\Phi(x) \cdot w\|^\vee \leqslant \left(k\bar{\lambda}_\ell + 2\varepsilon\right)\|w\|^\vee$.*

Proof. Suppose that $w = (u, v) \in C^+$, and let $(\tilde{u}, \tilde{v}) = D\Phi(x) \cdot (u, v)$ as before. We have $\|(u, v)\|^\vee = \|u\|$ and since, by lemma 4.5, $(\tilde{u}, \tilde{v}) \in C^+$, we also have $\|(\tilde{u}, \tilde{v})\|^\vee = \|\tilde{u}\|$. Hence inequality (16) (with n is chosen as before) can be rewritten as

$$\|(\tilde{u}, \tilde{v})\|^\vee \geqslant \left(k\bar{\lambda}_{\ell-1} - 2\varepsilon\right)\|(u, v)\|^\vee.$$

Now suppose that $(u, v) \in \left(D\Phi(x)\right)^{-1}C^- \subset C^-$, and once again let $(\tilde{u}, \tilde{v}) = D\Phi(x) \cdot (u, v) \in C^-$. In this case, we have $\|(u, v)\|^\vee = \|v\|$ and $\|(\tilde{u}, \tilde{v})\|^\vee = \|\tilde{v}\|$. Inequality (17) still holds, but not (18), which is replaced by

$$\|(\tilde{u}, \tilde{v})\|^\vee = \|\tilde{v}\| \leqslant \left(k\bar{\lambda}_\ell + 2\varepsilon\right)\|v\| = \left(k\bar{\lambda}_\ell + 2\varepsilon\right)\|(u, v)\|^\vee. \quad \square$$

Propositions 4.1 and 4.2 follow from the lemmas above and standard arguments (see, for instance, [21, proposition 6.2.12]).

5. Some topological and measure-theoretic considerations

Section 4 contains the beginning of a hyperbolic theory for CMNs of the type studied in this paper. The relatively simple analysis there, however, does not tell the whole story. The maps $\Phi = A_C \circ F$ are *piecewise* (partially) hyperbolic and not necessarily one-to-one; moreover, the discontinuity sets, which are determined by the coupling graphs, occur in a particular way. This combination of hyperbolic and discontinuous behavior leads to interesting and nontrivial geometric and dynamical properties. In a forthcoming article, the first-named author will discuss the ergodic theory of some of these maps, including the existence of physical measures.

We finish here with a few observations that we hope will give the reader a glimpse into the range of possibilities these coupled networks are capable of exhibiting. Define the *attracting set* of $\Phi = A_C \circ F$ to be the set

$$\Lambda = \bigcap_{n=0}^{\infty} \overline{\Phi^n \left(\mathbb{T}^d \setminus \bigcup_{i=0}^{n-1} \Phi^{-i}(S) \right)}$$

where $S = F^{-1}\big(P(C)\big)$ is the singularity set for Φ, $\mathbb{T}^d \setminus \bigcup_{i=0}^{n-1} \Phi^{-i}(S)$ is the set on which Φ^n is defined, and the bar over the expression means closure. It follows from its definition that Λ is closed, $\Phi(\Lambda) = \Lambda$, and for all $x \in \mathbb{T}^d$ for which $\Phi^n x$ is defined for all $n \geqslant 0$, $\Phi^n x \to \Lambda$ as $n \to \infty$.

5.1. Measure and topology of Λ: easy observations

For definiteness, consider here local maps of the form $f_i(x) = kx + \varepsilon g_i(x) + b_i \bmod 1$. As in Section 4, we assume ε is small enough that they are local diffeomorphisms.

Proposition 5.1. *Let A_C be a coupling map and $\Phi = A_C \circ F$.*

(a) *If k is large enough (depending on C), then $\Lambda = \overline{A_C\big(\mathbb{T}^d \setminus P(C)\big)}$. In particular, Λ is the closure of its interior and has positive Lebesgue measure.*

(b) *If, on the other hand, $|\det D\Phi(x)| < 1$ for all $x \in X$, then Λ is nowhere dense and has Lebesgue measure zero.*

We may think of (a) as the case where the expansion is strong and coupling weak, while (b) corresponds to stronger coupling and not as strong expansion.

Proof. Since $A_C\big(\mathbb{T}^d \setminus P(C)\big)$ is an open set, $F\big(A_C\big(\mathbb{T}^d \setminus P(C)\big)\big) = \mathbb{T}^d$ if k is large enough. This proves (a). We leave the rest as an easy exercise. $\square$

5.2. Connectedness of Λ

In the regime of Proposition 5.1(a), Λ is the closure of $A_C\big(\mathbb{T}^d \setminus P(C)\big)$. We focus next on the connectedness of this set. Notice that $A_C\big(\mathbb{T}^d \setminus P(C)\big)$ is connected if and only if its closure is.

Proposition 5.2. *Let A_C be a coupling map and G its associated coupling graph.*

(a) *If G is a tree, then $A_C\big(\mathbb{T}^d \setminus P(C)\big)$ is connected.*

(b) If G contains a 3-cycle, then $A_C\big(\mathbb{T}^d \setminus P(C)\big)$ is not connected.

Proof. Since A_C is a homeomorphism onto its image, $A_C\big(\mathbb{T}^d \setminus P(C)\big)$ is connected if and only if $\mathbb{T}^d \setminus P(C)$ is connected, so we consider the latter. For the length of this proof, we consider $\mathbb{S}^1$ as the unit circle in $\mathbb{C}$, so that x and $-x \in \mathbb{S}^1$ are antipodal.

(a) It suffices to show that given any point $x \in \mathbb{T}^d \setminus P(C)$, there is a continuous path in $\mathbb{T}^d \setminus P(C)$ that starts at x and ends at a point in the diagonal Δ of $\mathbb{T}^d$. This implies immediately the assertion in (a) since Δ is connected and $\Delta \subset \mathbb{T}^d \setminus P(C)$. These paths are constructed by induction on the vertices of G:

To start, pick a leaf, i.e., a vertex of valence 1, of G (see e.g. [15]). We call it i, and let x_i be be corresponding coordinate of x. Suppose i is adjacent in G to the vertex j. We move x_i in $\mathbb{S}^1$ continuously along the shortest path to x_j until $x_i = x_j$. Such a path remains in $\mathbb{T}^d \setminus P(C)$ because no condition other than $x_i \neq -x_j$ is imposed on x_i. From this point on, x_i and x_j will *always* move together, so we may consider the graph obtained from G by deleting the vertex i and the edge (i, j). We replace the label "j" of vertex j with $(j, \{i, j\})$.

In general, let G' be the graph obtained from previous steps. We choose a leaf of G', and suppose it is labeled as (i, I), where $I = \{i_1, \ldots, i_m\}$. Suppose also that the adjacent vertex in G' is (j, J), where $J = \{j_1, \ldots, j_n\}$. We move the vertices in I in tandem along the shortest path to x_j. Once again the reader should check that such a path is legal. The graph G' is updated by deleting the leaf (i, I) and replacing (j, J) with $(j, I \cup J)$. Since G is finite, the process ends when G' is reduced to a single vertex, at which point all the coordinates of x are equal.

(b) We leave it to the reader to check that it suffices to prove the assertion for a system whose coupling graph is a 3-cycle: If $\mathbb{T}^3 \setminus P(C)$ is disconnected for this system, then any larger coupling graph with a 3-cycle embedded in it will automatically lead to a disconnected $\mathbb{T}^d \setminus P(C)$.

Let x_1, x_2, and x_3 be the coordinates of $x \in \mathbb{T}^3 \setminus P(C)$. For each location of x_1, x_2 can be anywhere in $\mathbb{S}^1$ except for $-x_1$, and for each admissible configuration of (x_1, x_2), x_3 can be anywhere other than $-x_1$ and $-x_2$. These two points partition the set of possible locations for x_3 into two disjoint arcs: the one containing x_1 and x_2 and the one that does not. In Figure 9, x_3 is in the latter. We move the 3 points continuously along $\mathbb{S}^1$ keeping all configurations admissible, and try to maneuver x_3 to the other component of $\mathbb{S}^1 \setminus \{-x_1, -x_2\}$. Using coordinates relative to x_1, we may assume x_1 is fixed at 0 (as shown). We see that x_2 is now confined to the upper half-circle: it cannot cross $-x_1$, and cannot cross x_1 either because that would force x_3 onto $-x_1$. With x_2 locked in this half-circle, x_3 cannot move out of its initial component of $\mathbb{S}^1 \setminus \{-x_1, -x_2\}$, proving that $\mathbb{T}^3 \setminus P(C)$ is not path connected, hence not connected. $\qquad\square$
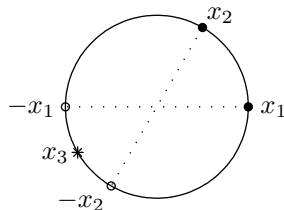
Figure 9. There is no admissible way to maneuver x_3 out of its component of $\mathbb{S}^1 \setminus \{-x_1, -x_2\}$, proving that $\mathbb{T}^3 \setminus P(C)$ is disconnected.

Thus in the situation of Proposition 5.1(a), for example, the attracting set Λ is disconnected. Notice that Λ becomes disconnected as soon as the coupling constants become positive, no matter how small, while for the uncoupled map, $\Lambda = \mathbb{T}^d$.

5.3. Decomposability of dynamics on Λ: an example

Disconnectedness of the attracting set does not in general imply decomposability of the dynamics, but that can happen as well. We present here an example in the strong coupling regime in which (i) Λ is disconnected, and (ii) the dynamics of Φ on Λ are not topologically transitive.

In this example, the local maps are $f(x) = 2x \bmod 1$, the coupling graph is a triangle, and the coupling strengths are all equal to some $\alpha \in \left(\frac{1}{4}, \frac{1}{3}\right)$ (the upper bound on α is from Section 3.2.1; the lower bound can be relaxed and is chosen to simplify the argument; see later). Thus Φ is piecewise linear, and by our choice of α, $D\Phi$ has a two-dimensional contracting (stable) subspace. As observed in Section 3.2.1, the diagonal $\Delta = \{x_1 = x_2 = x_3\} \subset \mathbb{T}^3$ is an invariant set on which Φ is expanding. Since every point on it has a 2-dimensional stable subspace, it follows immediately that Δ attracts all points in an open neighborhood. The attracting set Λ, however, is strictly larger than Δ. Figure 10 shows two other points, $x = (x_1, x_2, x_3) = (0, 1/3, -1/3)$ and $x' = (0, -1/3, 1/3)$, in Λ: Here $F(x) = x'$ and $F(x') = x$, and A_C leaves both points fixed. We will show that configurations of this type are also stable in a sense to be made precise.
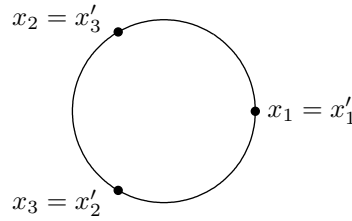

$x_2 = x'_3$

$x_1 = x'_1$

$x_3 = x'_2$

Figure 10. Examples of off-diagonal points in Λ.

The dynamical picture *vis a vis* the attracting set can be summarized as follows:

Proposition 5.3. *In the example above,*

(a) *Λ is the union of three disjoint circles Δ, Ξ_1 and Ξ_2, where Δ is the diagonal and Ξ_1 and Ξ_2 are symmetrically placed with respect to Δ and parallel to it;*

(b) *$\Phi(\Delta) = \Delta$, $\Phi(\Xi_1) = \Xi_2$, and $\Phi(\Xi_2) = \Xi_1$; Φ maps each circle as a degree 2 covering onto its image;*

(c) *every point in $\mathbb{T}^d \setminus \cup_{n \geqslant 0} \Phi^{-n}(S)$ is attracted to either Δ or $\Xi_1 \cup \Xi_2$; the basin of each of these two attractors includes an open neighborhood of the attractor.*

Proof. Our plan of proof is as follows: We will introduce new coordinates on $\mathbb{T}^3 \setminus P(C)$ with respect to which both A_C and F are product maps on a space $\mathcal{D} \times \mathbb{S}^1$ where $\mathcal{D}$ is a subset of a plane, $\mathbb{S}^1$ has length $\sqrt{3}$ (a benign abuse of notation) and the fiber maps Φ on $\mathbb{S}^1$ are degree 2 coverings. The problem is then reduced to studying how these maps act on the base $\mathcal{D}$. We will show that on $\mathcal{D}$, the forward limit set consists of exactly three points, corresponding to the three circles in the proposition.

Let $\mathbb{P} \subset \mathbb{R}^3$ be the plane through the origin orthogonal to $(1, 1, 1)^T$, and let $\mathcal{D}$ be the open subset of $\mathbb{P}$ with three connected components $\mathcal{D}_0$, $\mathcal{D}_1$, $\mathcal{D}_2$, each of which being

the interior (in $\mathbb{P}$) of the convex hull of the set of vectors shown (see Figures 11(b) and 12(a)). Here $a = \left(\frac{1}{2}, -\frac{1}{2}, 0\right)^T$, $b = \left(-\frac{1}{6}, -\frac{1}{6}, \frac{1}{3}\right)^T$, $c = (a+b)/2$ and $d = (a-b)/2$. We now introduce a mapping $\psi : \mathcal{D} \times \mathbb{S}^1 \to \mathbb{T}^3 \setminus P(C)$ that will be the coordinate change in the first paragraph.

Claim. *Denoting coordinates on $\mathcal{D} \times \mathbb{S}^1$ by $(\tilde{x}, \rho)$ and letting $(\,\cdot\,)_i$ be the i-th (Cartesian) coordinate in $\mathbb{R}^3$, we let $\psi : \mathcal{D} \times \mathbb{S}^1 \to \mathbb{T}^3 \setminus P(C)$ be the mapping given by*

$$\left(\psi(\tilde{x}, \rho)\right)_i = \left(\tilde{x} + \tfrac{1}{\sqrt{3}} \rho \cdot (1, 1, 1)^T\right)_i \quad \mod 1.$$

Then ψ is a volume-preserving bijection.

Rather than giving a formal proof, it is more interesting to show how $\mathbb{T}^3 \setminus P(C)$ can be broken up and "reassembled" into $\mathcal{D} \times \mathbb{S}^1$. The set $\mathbb{T}^3 \setminus P(C)$ is illustrated in Figure 11(a), where the shaded planes represent $P(C)$, and the thick line represents the diagonal connecting the origin to $(1, 1, 1)^T$. The unit cube representing $\mathbb{T}^3$ is broken up *along* $P(C)$ and reassembled (respecting the identifications on the faces of the cube) into a intermediate object resembling the solid in Figure 11(b) but with a jagged top and bottom. If we take each line segment parallel to $(1, 1, 1)^T$ in this intermediate object and rigidly slide it in the direction parallel to $(1, 1, 1)^T$ until its lower end touches $\mathbb{P}$, we get Figure 11(b) exactly. These translations leave $\mathbb{T}^3 \setminus P(C)$ invariant, since the line segments correspond to circles inside $\mathbb{T}^3$ that do not intersect $P(C)$. (To see step-by-step illustrations of this process, see `www.impa.br/~koiller/reassembly.html`.) A quick check shows that the area of $\mathcal{D}$ is $\sqrt{3}/3$ and $|\det D\psi| = 1$, so $\mathcal{D} \times \mathbb{S}^1$ has the correct volume.


(a)   (b)
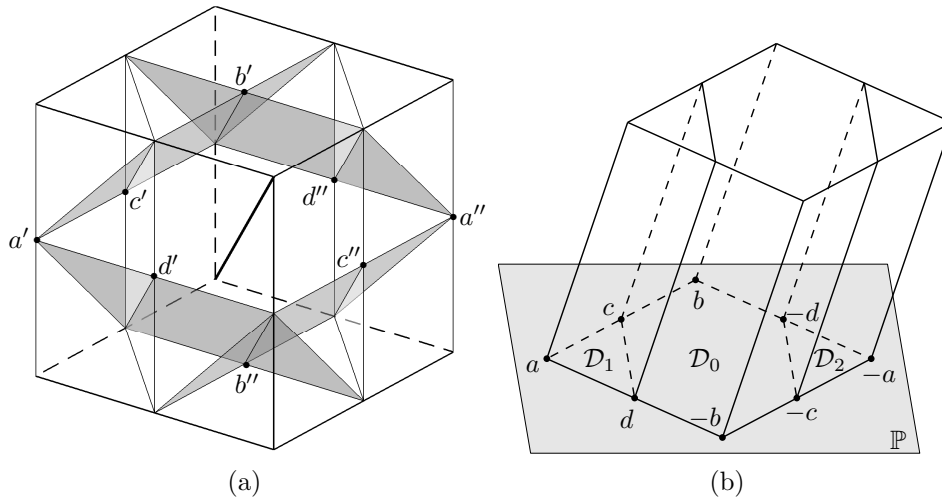
Figure 11. Two representations of the set $\mathbb{T}^3 \setminus P(C)$ in $\mathbb{R}^3$. The points x' in (a) are projected orthogonally to the points $x \in \mathbb{P}$ in (b), while the x'' are projected to $-x$.

The $(\tilde{x}, \rho)$ coordinates can be understood intuitively as follows. Let $\mathcal{D} \times \mathbb{S}^1$ be identified with a subset of $\mathbb{R}^3$ in the canonical way, i.e., $\mathcal{D} \times \{0\}$ is identified with $\mathcal{D} \subset \mathbb{P}$, and $\mathbb{S}^1$-fibers are orthogonal to $\mathbb{P}$. The resulting subset of $\mathbb{R}^3$ as shown in Figure 11(b) is a representation of $\mathbb{T}^3 \setminus P(C)$. With $\mathcal{D} \times \mathbb{S}^1$ seen in this way, the map

$\pi : \mathcal{D} \times \mathbb{S}^1 \to \mathcal{D}$, $\pi(\tilde{x}, \rho) = \tilde{x}$, is the projection onto $\mathcal{D} \subset \mathbb{P}$ along $\mathbb{S}^1$-fibers. Notice that the boundary $\partial \mathcal{D}$ would have been the image of $P(C)$ under this projection except that this set is not in $\mathcal{D}$. It is important to note that *for $x \in P(C)$, the $\mathbb{S}^1$-fiber through x lies entirely in $P(C)$.*

We leave it to the reader to check that both $\psi^{-1} \circ A_C \circ \psi$ and $\psi^{-1} \circ F \circ \psi$ (wherever it is defined) preserve the $\mathbb{S}^1$-fibers in $\mathcal{D} \times \mathbb{S}^1$, and that the fiber maps are degree two coverings as claimed. Let $\tilde{\Phi}$, $\tilde{A}_C$ and $\tilde{F}$ be the induced maps on $\mathcal{D}$, defined on their respective domains. It remains to study the limit set of $\tilde{\Phi} = \tilde{A}_C \circ \tilde{F}$. As we will see, it is simpler to look at iterations of $\tilde{F} \circ \tilde{A}_C$ rather than $\tilde{A}_C \circ \tilde{F}$. We will show that $\tilde{F} \circ \tilde{A}_C$ is a contraction taking $\mathcal{D}$ into itself, its successive images converging to three points. That $\tilde{\Phi}^n(\mathcal{D})$ will converge to the same 3 points then follows easily.

Leaving out (straightforward) computational details, we claim that $\tilde{A}_C$ is a piecewise linear contracting map that sends each $\mathcal{D}_i$ into itself, contracting equally in all directions by $2 - 6\alpha$ (see Section 3.2.1). Moreover, it leaves the centers of each $\mathcal{D}_i$, denoted ξ_i, fixed. See Figure 12(a,b). Now $\tilde{F}$ expands all directions by 2, but our lower bound on α was chosen so that $\tilde{A}_C$ is sufficiently contracting that $\tilde{F}(\tilde{A}_C(\mathcal{D})) \subset \mathcal{D}$. Denoting $\mathcal{D}_i' = \tilde{A}_C(\mathcal{D}_i)$, we have $\tilde{F}(\mathcal{D}_0') \subset \mathcal{D}_0$, $\tilde{F}(\mathcal{D}_1') \subset \mathcal{D}_2$ and $\tilde{F}(\mathcal{D}_2') \subset \mathcal{D}_1$. Moreover, $\tilde{F}(\xi_0) = \xi_0$, $\tilde{F}(\xi_1) = \xi_2$ and $\tilde{F}(\xi_2) = \xi_1$. See Figure 12(b,c). The map $\tilde{\Theta} = \tilde{F} \circ \tilde{A}_C$, which is overall piecewise contracting, is seen by going from (a) to (c) in Figure 12. It is now clear that the attracting set for $\tilde{\Theta}$ consists of the points ξ_i, $i = 0, 1, 2$.
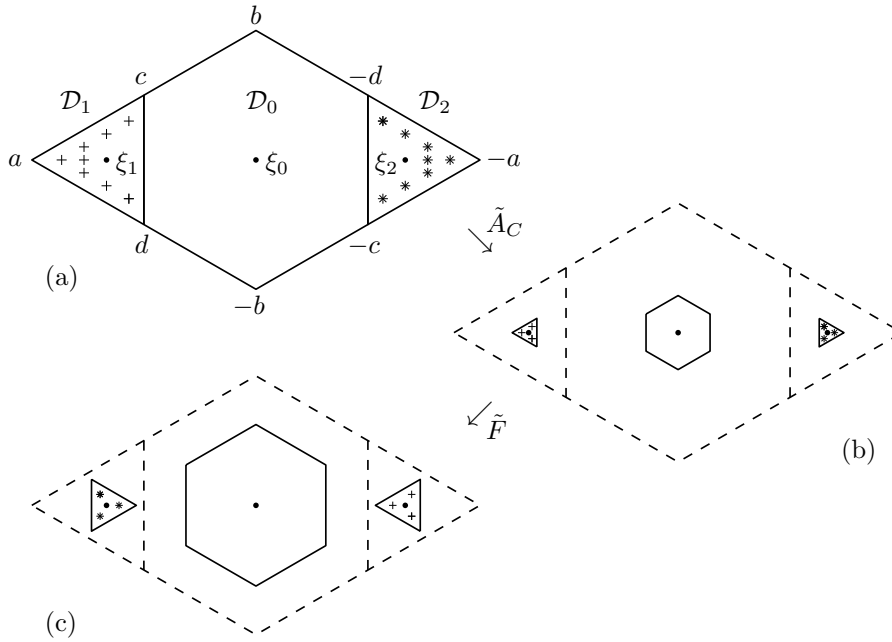
Figure 12. Each $\mathcal{D}_i$ is contracted and mapped into itself under $\tilde{A}_C$. Call the images $\mathcal{D}_i'$. Under $\tilde{F}$, $\mathcal{D}_1'$ is expanded and moved rigidly from $\mathcal{D}_1$ to $\mathcal{D}_2$; similarly, $\mathcal{D}_2'$ is expanded and moved from $\mathcal{D}_2$ to $\mathcal{D}_1$. (The figures are not to scale.)

The assertions in Proposition 5.3 are obtained by interpreting the results above back to $\mathbb{T}^3$. $\qquad\square$

Acknowledgments

The first-named author would like to thank Professor Enrique Pujals for useful comments and suggestions.

References

[1] Afraimovich V S and Chow S-N 1995 Topological spatial chaos and homoclinic points of $\mathbb{Z}^d$-action in lattice dynamical systems *Japan J. Indust. Appl. Math.* **12** 367–83
[2] Afraimovich V S, Chow S-N and Shen W 1996 Hyperbolic homoclinic points on $\mathbb{Z}^d$-action in lattice dynamical systems *Internat. J. Bifur. Chaos Appl. Sci. Engrg.* **6** 1059–75
[3] Afraimovich V S and Courbage M 2000 On the abundance of traveling waves in coupled expanding circle maps. *Amer. Math. Soc. Transl., Series 2* 200 15–21
[4] Bardet J-B and Keller G 2006 Phase transitions in a piecewise expanding coupled map lattice with linear nearest neighbour coupling *Nonlinearity* **19** 2193–210
[5] Bardet J-B, Gouëzel S and Keller G 2007 Limit theorems for coupled interval maps *Stoch. Dyn.* **7** 17–36
[6] Bunimovich L A 1995 Coupled map lattices: one step forward and two steps back *Physica D* **86** 248–55
[7] Bunimovich L A and Sinai Ya G 1988 Spacetime chaos in coupled map lattices *Nonlinearity* **1** 491–516
[8] Bunimovich L A, Sinai Ya G and Chernov N I 1990 Markov partitions for two-dimensional hyperbolic billiards *Russian Math. Surveys* **45** 105–52
[9] Bunimovich L A, Sinai Ya G and Chernov N I 1991 Statistical properties of two-dimensional hyperbolic billiards *Russian Math. Surveys* **46** 47–106
[10] Buzzi J 2000 Absolutely continuous invariant probability measures for arbitrary expanding piecewise $\mathbb{R}$-analytic mappings of the plane *Ergodic Theory Dynam. Systems* **20** 697–708
[11] Chazottes J-R and Fernandez B (editors) 2005 *Dynamics of Coupled Map Lattices and of Related Spatially Extended Systems* (Lecture Notes in Physics **671**) (Berlin: Springer)
[12] Coutinho R, Fernandez B and Guiraud P 2008 Symbolic dynamics of two coupled Lorenz maps: from uncoupled regime to synchronization *Physica D* **237** 2444–62
[13] Cowieson W J 2000 Stochastic stability for piecewise expanding maps in $\mathbb{R}^d$ *Nonlinearity* **13** 1745–60
[14] Cowieson W J 2002 Absolutely continuous invariant measures for most piecewise smooth expanding maps *Ergodic Theory Dynam. Systems* **22** 1061–78
[15] Diestel R 1997 *Graph Theory* (Graduate Texts in Mathematics **173**) (New York: Springer)
[16] Góra P and Boyarsky A 1989 Absolutely continuous invariant measures for piecewise expanding C^2 transformations in $\mathbb{R}^n$ *Israel J. Math.* **67** 272–86
[17] Hasselblatt B and Katok A (editors) 2006 *Handbook of Dynamical Systems* volume 1B (Amsterdam: Elsevier)
[18] Jiang M and Pesin Ya B 1998 Equilibrium measures for coupled map lattices: existence, uniqueness and finite-dimensional approximations *Comm. Math. Phys.* **193** 675–711
[19] Kaneko K 1984 Period doubling of kink-antikink patterns, quasiperiodicity in antiferro-like structures and spatial intermittency in coupled map lattices *Progr. Theoret. Phys.* **72** 480–86
[20] Kaneko K 1985 Spatial Period-doubling in Open Flow *Physics Letters* **111** 321–25
[21] Katok A and Hasselblatt B 1995 *Introduction to the Modern Theory of Dynamical Systems* (Cambridge: Cambridge University Press)
[22] Keller G, Künzle M and Nowicki T 1992 Some phase transitions in coupled map lattices *Physica D* **59** 39–51
[23] Keller G and Liverani C 2004 Coupled map lattices without cluster expansion *Discrete Contin. Dyn. Syst.* **11** 325–35
[24] Keller G and Liverani C 2006 Uniqueness of the SRB measure for piecewise expanding weakly coupled map lattices in any dimension *Comm. Math. Phys.* **262** 33–50
[25] Kuznetsov S P 1983 On critical behavior of one-dimensional lattices *Pis'ma v Zhurnal Tekhnicheskoi Fiziki* **9** 94–98 (in Russian)
[26] Lax P D 1997 *Linear Algebra* (New York: Wiley-Interscience)
[27] Liverani C and Wojtkowski M P 1995 *Ergodicity in Hamiltonian Systems (Dynamics Reported, New Series, volume 4)* (Berlin: Springer) 130–202
[28] Pesin Ya B and Sinai Ya G 1991 Space-time chaos in chains of weakly interacting hyperbolic mappings *Adv. Soviet Math.* **3** 165–98

[29] Petersen K 1983 *Ergodic Theory* (Cambridge: Cambridge University Press)
[30] Saussol B 2000 Absolutely continuous invariant measures for multidimensional expanding maps
        Israel J. Math. **116** 223–48
[31] Sinai Ya G 1970 Dynamical systems with elastic reflections. Ergodic properties of dispersing
        billiards *Russian Math. Surveys* **25** 137–89
[32] Waller I and Kapral R 1984 Spatial and temporal structure in systems of coupled nonlinear
        oscillators *Physical Review* A **30** 2047–55